40TH IAHR WORLD CONGRESS VIENNA–AUSTRIA
21–25 AUGUST 2023
FROM MOUNTAINS TO COAST

Proceedings of the 40th IAHR World Congress
21-25 August 2023
Vienna, Austria
DOI number

Using a Boussinesq-type 1-D model to simulate Favre waves

Bastien Jouy[1,2], D. Violeau[1,2], M. Ricchiuto[3], M. Le[2], E. Demay[1]

[1] Electricité de France R&D / Laboratoire National d'Hydraulique et Environnement, Chatou, France
[2] Laboratoire d'Hydraulique Saint-Venant, Chatou, France
[3] Team CARDAMOM / Inria Bordeaux, Talence, France

Abstract

In this paper, we propose a reformulation of the Winckler-Liu model (2015), which belongs to the family of Boussinesq-type models, allowing the modeling of weakly dispersive, weakly nonlinear waves in channels of arbitrary cross-sections, even when the cross-section varies significantly within a wavelength. A decoupling of the elliptical part modeling non-hydrostatic effects from the hyperbolic part identical to the shallow water equations, is performed. This allows an easier numerical implementation in an existing code. The model is verified with an analytical solitary wave solution derived for a prismatic channel of rectangular cross-section.

Keywords: Boussinesq-type equations, Weakly dispersive nonlinear waves, Solitary wave, Favre waves, Numerical methods

1. INTRODUCTION

The Favre waves occur upstream dam sluice gate after their sudden closure. They propagate upstream and take the form of an undular bore as long as the upstream Froude number is less than a critical value close to 1.3 (for larger Froude number they disappear in favor of an ordinary mobile hydraulic jump). As nonlinear, weakly dispersive wave train, the Favre waves cannot be modeled with the shallow water equations; they require appropriate set of equations such as Serre or Boussinesq-type equations.

Willing to perform numerical simulations of these waves for the purpose of industrial applications, we aim at establishing a numerical model. One of the main difficulties is that real-world hydropower channels mostly have trapezoidal cross sections. We thus aim at building a model capable of handling arbitrary cross-sectional nonlinear, weakly dispersive channel water waves. Looking at the existing appropriate theories in the literature, we found that most models only allow treating the prismatic channel cases (Peregrine, 1968) or slowly varying cross-sectional channels (Teng and Wu, 1992). We thus focus on a more recent model allowing arbitrary space variations of the channel cross section, proposed by Winckler and Liu (2015), though in this paper we will mainly address the prismatic case, for which Winckler and Liu's model renders Peregrine's one.

In order to write an appropriate numerical scheme of the Winckler-Liu model, we will reformulate it in a conservative form, with dispersive terms treated as a specific operator applied to an auxiliary variable. The latter will be found by solving an elliptic equation. This hyperbolic-elliptic approach is traditional in the numerical treatment of dispersive water wave equations (see e.g. Filippini et al. (2016)). We will present a numerical scheme for the resulting system, as well as a verification case based on an exact analytic solution taking the form of a solitary wave.

2. GOVERNING EQUATIONS

2.1 Original Winckler-Liu model

Winckler and Liu (2015)'s model for weakly nonlinear, weakly dispersive channel waves reads

$$\eta_t + \frac{1}{B_0}(A_0 u)_x - \epsilon\frac{B_0'}{B_0^2}\eta(A_0 u)_x + \frac{\epsilon}{B_0}\eta(B_0 u\eta)_x = O(\epsilon^2, \epsilon\mu^2, \mu^2) \quad [1]$$

$$u_t + \epsilon u u_x + g\eta_x + \mu^2(\alpha u_t + \beta u_{tx} + \gamma u_{txx}) = O(\epsilon^2, \epsilon\mu^2, \mu^4) \quad [2]$$

where $\eta(x,t)$ and $u(x,t)$ denote the width-averaged free-surface elevation and the cross-sectional averaged velocity, respectively; x and t are the space and time coordinates and subscripts refer to partial derivatives; A_0 and B_0 are the rest cross-section area and rest free-surface width, respectively (see Fig. 1). The nonlinearity and dispersion are quantified by the small, dimensionless parameters ϵ and μ, respectively.

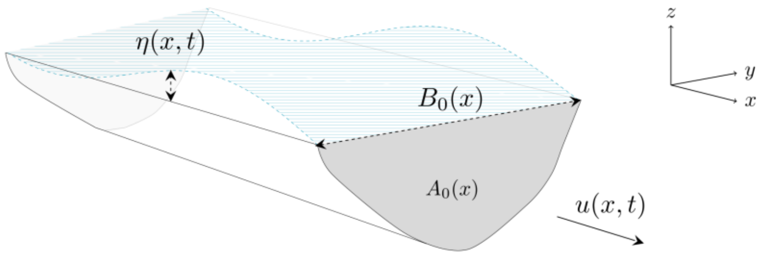

Figure 1. Notation.

The shape of the channel cross-section is contained in the shape parameters α, β and γ. They are defined as solutions to boundary value problems on the rest cross-section (see Winckler and Liu, 2015 for more details).

2.2 Hyperbolic elliptic reformulation

We rewrite equations [1], [2] in the following form, obtained with a bit of algebra:

$$\begin{cases} (1+\mu^2\mathcal{T})\Phi = -H_x \\ A_t + \epsilon(Au)_x = 0 \\ (Au)_t + \epsilon(Au^2) + gA\eta_x = A\Phi + AH_x \end{cases} \quad [3]$$

where A is the cross-section area. Moreover, $\mathcal{T}$ is the differential operator defined by

$$\mathcal{T} \doteq \alpha \mathrm{I} + \beta^* \partial_x - \partial_x(\gamma^* \partial_x) \quad [4]$$

with $\beta^* \doteq \beta + \gamma_x^*$ and $\gamma^* \doteq -\gamma$. The right-hand side of the last line in [3] contains dispersive terms; H_x is the space derivative of the hydrostatic head $H = \epsilon u^2/2 + gh$, while the auxiliary variable Φ is the solution to the elliptic equation in the first line of [3].

In the particular case of a prismatic channel (i.e. having uniform cross section with x) with rectangular cross-section and without bathymetry, $\alpha = \beta = 0$ and $\gamma^* = h_0^2/3 = cst$; denoting h_0 the rest water depth. The above equations simplify as follows:

$$\begin{cases} (1+\mu^2\mathcal{T})\Phi = -H_x \\ h_t + \epsilon(hu)_x = 0 \\ (hu)_t + \left(\epsilon hu^2 + \frac{1}{2}gh^2\right) = h\Phi + hH_x \end{cases} \quad [5]$$

h being the water depth, and

$$\mathcal{T} = -\gamma^* \partial_{xx} \quad [6]$$

2.3 Analytic solitary wave

For a prismatic channel of rectangular section, the system [5], [6] has solutions as travelling waves, i.e. waves propagating at a constant velocity c with a constant shape. The particular case of solitary waves is given by a pseudo-elliptic integral:

$$\frac{x-ct}{h_0} = \mu \int_{\frac{h}{h_0}}^{1+\epsilon} \frac{\mathrm{d}\zeta}{\sqrt{2\zeta^4 - 3\zeta^3 + \zeta - \frac{6\epsilon}{F_0^2}\left(\ln\zeta + \frac{1}{\zeta} - 1\right)\zeta^4}} \quad [7]$$

ζ being a dummy variable and F_0 a Froude number:

$$F_0 \doteq \frac{c}{\sqrt{gh_0}} \tag{8}$$

It is worth noting that the solution to the original system [1], [2] is much more complicated (Teng, 1999). Winckler and Liu (2015) give an approximate solution but the above one is exact; this is due to our continuity equation which is written in the exact shallow water form. The integral [7] can be plotted using an appropriate quadrature method and depicted on Fig. 2.

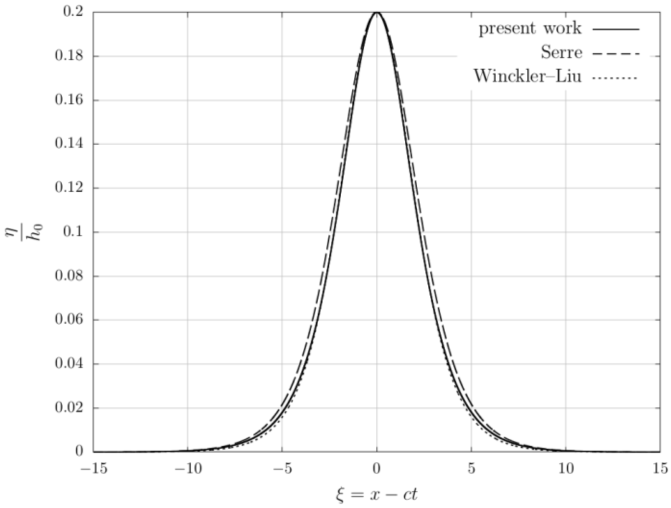

Figure 2. Solitary wave profiles: comparison of our equation [7] against the classical Serre solution (Serre, 1953) and the Winckler and Liu (2015) approximation, for the amplitude $\epsilon = 0.2$.

3. NUMERICAL IMPLEMENTATION AND TESTS

3.1 Numerical choices

First the elliptic equation is solved with a classical finite element method with piecewise linear polynomials, as example for Φ:

$$\Phi = \sum_{j=1}^{N} \varphi_i \, \Phi_i \tag{9}$$

where φ_i denote hat shaped basis function and Φ_i the value of Φ at node i. Considering prismatic channel with rectangular cross-section, the linear solving system associated to the elliptic equation in [5] is:

$$\sum_{i=1}^{N} a(\varphi_i, \varphi_j)\Phi_i = \sum_{i=1}^{N} b(\varphi_j) \tag{10}$$

with the following matrix:

$$a(\varphi_i, \varphi_j) = \gamma^* \int_\Omega \partial_x \varphi_i \, \partial_x \varphi_j \, \mathrm{d}x \tag{11}$$

and,

$$b(\varphi_j) = -\left(\int_\Omega \partial_x \varphi_i \varphi_j \, \mathrm{d}x\right) H_j - (\gamma^* \Phi_x \varphi_j)|_{\partial\Omega} \tag{12}$$

where in this case $\gamma^* = h_0^2/3$ and the boundary terms are treated in a way that yields to the Saint-Venant equations.

Once the linear system [10] is solved, the hyperbolic equations in [6] can be treated, considering Φ by adding source term and can be written in the following form:

$$\boldsymbol{U}_t + \boldsymbol{F}(\boldsymbol{U})_x = \boldsymbol{S}(\boldsymbol{U}) \quad [13]$$

with

$$\boldsymbol{U} = \begin{pmatrix} h \\ hu \end{pmatrix}, \boldsymbol{F}(\boldsymbol{U}) = \begin{pmatrix} hu \\ hu^2 + gh^2 \end{pmatrix}, \boldsymbol{S}(\boldsymbol{U}) = \begin{pmatrix} 0 \\ hH_x + h\Phi \end{pmatrix} \quad [14]$$

Denoting the cell $\left[x_{i-\frac{1}{2}}, x_{i+\frac{1}{2}}\right]$, and the constant grid size $\Delta x = x_{i+\frac{1}{2}} - x_{i-\frac{1}{2}}$; the cell averaged of $\boldsymbol{U}$ is:

$$\boldsymbol{U}_i^n = \frac{1}{\Delta x}\int_{x_{i-\frac{1}{2}}}^{x_{i+\frac{1}{2}}} \boldsymbol{U}(x, t^n)\,\mathrm{dx} \quad [15]$$

with t^n the time at iteration n. A finite volume method (FVM) applied to system [13] is highly inspired from Filippini et al. (2016) and can be written as follows:

$$\boldsymbol{U}_i^{n+1} = \boldsymbol{U}_i^n - \frac{\Delta t}{\Delta x}\left(\boldsymbol{F}_{i+\frac{1}{2}} - \boldsymbol{F}_{i-\frac{1}{2}}\right) + \frac{\Delta t}{\Delta x}\Delta \boldsymbol{S}_{H,i} + \Delta t \overline{\boldsymbol{S}}_{\Phi} \quad [16]$$

where $\Delta t = t^{n+1} - t^n$ is the time step, $\boldsymbol{F}_{i\pm 1/2}$ and $\Delta \boldsymbol{S}_{H,i}$ denote numerical fluxes and the source term involving the derivative of the hydrostatic head at the interfaces, respectively. A centered treatment is applied to the term involving the variable of the elliptic equation $\overline{\boldsymbol{S}}_{\Phi}$. Numerical fluxes are written with a Roe (1981) scheme:

$$\boldsymbol{F}_{i+\frac{1}{2}} = \frac{1}{2}\left[\boldsymbol{F}\left(\boldsymbol{U}_{i+\frac{1}{2}}^L\right) + \boldsymbol{F}\left(\boldsymbol{U}_{i+\frac{1}{2}}^L\right)\right] - \frac{1}{2}|\mathbf{A}|_{i+\frac{1}{2}}\Delta \boldsymbol{U}_{i+\frac{1}{2}} \quad [\mathbf{17}]$$

where $\Delta \boldsymbol{U}_{i+1/2} = \boldsymbol{U}_{i+1/2}^R - \boldsymbol{U}_{i+1/2}^L$ denote the jump in $\boldsymbol{U}$ through the interface $i + 1/2$ and $\mathbf{A}_{i+1/2}$ is the Jacobian matrix of the system [13] in the Roe average state which is equal to:

$$\boldsymbol{A}_{i+\frac{1}{2}} = (\boldsymbol{P}\boldsymbol{\Lambda}\boldsymbol{P}^{-1})_{i+\frac{1}{2}} \quad [18]$$

with the eigenvectors matrices $\boldsymbol{P}$ and the diagonal matrix of eigenvalues $\boldsymbol{\Lambda}$. The upwinding source term in [16] can be expressed as:

$$\Delta \boldsymbol{S}_{H,i} = \boldsymbol{S}_{H,i+\frac{1}{2}}^{-}\left(\boldsymbol{U}_{i+\frac{1}{2}}^L, \boldsymbol{U}_{i+\frac{1}{2}}^R\right) + \boldsymbol{S}_{H,i-\frac{1}{2}}^{+}\left(\boldsymbol{U}_{i-\frac{1}{2}}^L, \boldsymbol{U}_{i-\frac{1}{2}}^R\right) + \boldsymbol{S}_{H,i}^{*}\left(\boldsymbol{U}_{i+\frac{1}{2}}^L, \boldsymbol{U}_{i-\frac{1}{2}}^R\right) \quad [19]$$

where

$$\boldsymbol{S}_{H,i+\frac{1}{2}}^{-}\left(\boldsymbol{U}_{i+\frac{1}{2}}^L, \boldsymbol{U}_{i+\frac{1}{2}}^R\right) = \frac{1}{2}[\boldsymbol{P}(\boldsymbol{I} - \boldsymbol{\Lambda}^{-1}|\boldsymbol{\Lambda}|)\boldsymbol{P}^{-1}]_{i+\frac{1}{2}}\tilde{\boldsymbol{S}}_{H,i+\frac{1}{2}} \quad [20]$$

$$\boldsymbol{S}_{H,-\frac{1}{2}}^{+}\left(\boldsymbol{U}_{i-\frac{1}{2}}^L, \boldsymbol{U}_{i-\frac{1}{2}}^R\right) = \frac{1}{2}[\boldsymbol{P}(\boldsymbol{I} + |\boldsymbol{\Lambda}|)\boldsymbol{P}^{-1}]_{i-\frac{1}{2}}\tilde{\boldsymbol{S}}_{H,i-\frac{1}{2}} \quad [21]$$

$\boldsymbol{I}$ denoting the identity matrix, and

$$\tilde{\boldsymbol{S}}_{H,i+\frac{1}{2}} = \begin{bmatrix} 0 \\ \frac{h^L + h^R}{2}\left(H^R - H^L\right) \end{bmatrix}_{i+\frac{1}{2}} \quad [22]$$

with a similar expression for $\tilde{\boldsymbol{S}}_{H,i-1/2}$. The last term in [19] is a centered correction assuring well-balance property of the scheme when using higher order reconstructions of the variables in the cell. In the present work, both 1st-order and 2nd-order schemes are used with for the latter a classical MUSCL piecewise linear reconstruction. This correction term guaranteeing steady state solutions is as follows:

$$\boldsymbol{S}^{*}_{H,i}\left(\boldsymbol{U}^{L}_{i+\frac{1}{2}},\boldsymbol{U}^{R}_{i-\frac{1}{2}}\right)=\begin{bmatrix}0\\ \frac{h^{L}_{i+\frac{1}{2}}+h^{R}_{i-\frac{1}{2}}}{2}\left(H^{L}_{i+\frac{1}{2}}-H^{R}_{i-\frac{1}{2}}\right)\end{bmatrix} \quad [23]$$

The discretization of the source term $\overline{\boldsymbol{S}}_{\Phi}$ in [16] can be written as:

$$\overline{\boldsymbol{S}}_{\Phi}=\frac{1}{8}\begin{bmatrix}0\\ h^{L}_{i+\frac{1}{2}}(\Phi_{i+1}+3\Phi_{i})+h^{R}_{i-\frac{1}{2}}(3\Phi_{i}+\Phi_{i-1})\end{bmatrix} \quad [24]$$

The node corresponding to the space discretization of the elliptic equation coincide with the cell node in the FVM. Second order in time is performed using Heun method to get a complete 2nd order accuracy scheme in time-space.

3.2 Verification with the solitary wave solution

Both the elliptic and the hyperbolic phase solving were verified independently using manufactured solutions while the verification of the coupling is performed with the solitary wave solutions derived [7]. For the verification case, the domain is $x\in[-12\lambda,12\lambda]$, where the solitary wave is initialized at $x=0$, with an amplitude corresponding to a nonlinearity parameter $\epsilon=0.2$. The boundary conditions are derived from the exact solution [7]. Analytical and numerical solutions are compared when the soliton has travelled 6.5 times its wavelength λ, with both the first and second order accuracy schemes. These solutions are plotted in Fig. 3 for a number of cells $N=8000$. An important numerical diffusion is observed for the soliton computed with first order FVM scheme while for the second order a quasi-superposition of the numerical and analytical solution is observed. For the convergence study we are interested in the L^2-norm error and we see from Fig. 4 that the resolution is in good agreement with the theoretical slopes corresponding to a convergence speed of order 1 and 2.

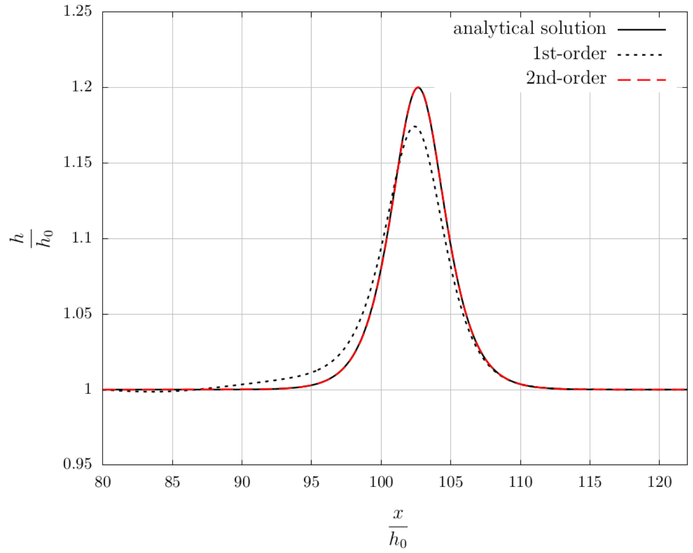

Figure 3. Analytical and simulated solitary waves for the amplitude $\epsilon=0.2$ at $t=\frac{6.5\lambda}{c}$ and $N=8000$ cells with first and second order accuracy FVM.

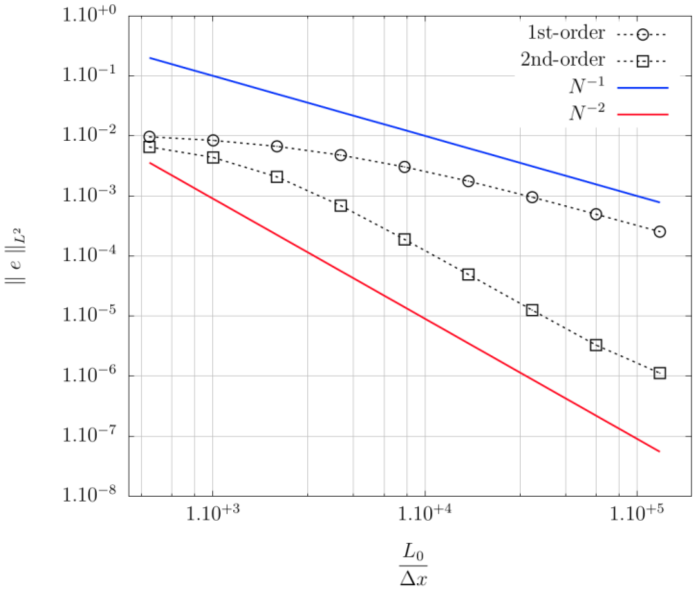

Figure 4. Convergence study of the L^2-norm error between analytical and simulated solitary waves for the amplitude $\epsilon = 0.2$, at $t = \frac{6.5\lambda}{c}$ for the first and second order accuracy FVM.

4. CONCLUSIONS

The present reformulation of Winckler and Liu system allowed both to put their equations in a conservative form while keeping the exact continuity equation. Moreover, the hyperbolic-elliptic decoupling allows an easier numerical treatment of the non-hydrostatic terms since one can keep the shallow water part of an existing code. As a first verification, a numerical scheme has been proposed for the resolution of this system in the case of a prismatic channel with rectangular cross-section and without bathymetry. Numerical results show a good solving of the solitary wave when the hyperbolic and elliptic problems are treated with a second order accuracy scheme, allowing the wave to preserve shape and amplitude during its propagation.

The present work is a promising starting point for the numerical modelling of nonlinear and weakly dispersive waves in prismatic channels of rectangular cross-section. The treatment of variable channel geometry, which Winckler–Liu model is normally designed for, is reserved for future studies.

5. ACKNOWLEDGEMENTS

Bastien Jouy expresses his gratitude for the financial support provided by the French ANRT (Association Nationale de la Recherche et de la Technologie) with the CIFRE Grant 2021/1094 towards his Ph.D. research program.

6. REFERENCES

Filippini, A.G., Kazolea, M., Ricchiuto M. (2016). A flexible genuinely nonlinear approach for nonlinear wave propagation, breaking and run-up. *Journal of Computational Physics,* 310, 381-417.
Peregrine, D.H. (1968). Long waves in a uniform channel of arbitrary cross-section. *Journal of Fluid Mechanics,* 32 (2), 353-365.
Roe, P.L. (1981). Approximate Riemann solvers, parameter vectors, and difference schemes. *Journal of Computational Physics,* 43, 357-372.
Serre, F. (1953). Contribution à l'étude des écoulements permanents et variables dans les canaux. *La Houille Blanche,* 39 (6), 830-872.
Teng, M.H., Wu, T.Y. (1992). Nonlinear water waves in channels of arbitrary shape. *Journal of Fluid Mechanics,* 242, 211-233.
Winckler, P., Liu, P.L.-F. (2015). Long waves in a straight channel with non-uniform cross-section. *Journal of Fluid Mechanics,* 770, 156-188.